

DESY SUMMER STUDENT PROJECT



Bc. Zuzana Birčáková

(DESY summer student 2010)

Date of birth:

March 10, 1988

Nationality:

Slovak

Study of thermal expansion of cryomilled $\text{Co}_{56}\text{Fe}_{16}\text{Zr}_8\text{B}_{20}$ alloy using hard X-rays

Area of research:

Photon Physics, Material Science

Time frame:

July 19 – September 10, 2010



Supervisor:

Dr. Jozef Bednarcík

Deutsches Elektronen Synchrotron DESY

Notkestr. 85

22607 Hamburg, Germany

email: jozef.bednarcik@desy.de

phone: +49-40-89981861

Short description of the research project

The objective of this project was to study the influence of cryomilling on thermal stability of an amorphous $\text{Co}_{56}\text{Fe}_{16}\text{Zr}_8\text{B}_{20}$ alloy using in-situ high-energy X-ray diffraction measurements. Particularly the thermal dependences of relative volume changes for an amorphous and a crystalline phase were being investigated. X-ray diffraction experiments using high-energy photons (100 keV) were performed at the BW5 wiggler beamline of DORIS III positron storage ring at DESY.



Contents

1	Introduction	1
2	Goals of the research project	2
3	Experimental part	2
3.1	Preparation of samples	2
3.2	High-energy X-ray diffraction at BW5	2
3.3	Data treatment	4
4	Results and Discussion	5
5	Conclusions	7
	Acknowledgement	7
	References	8

1 Introduction

An amorphous metal is a material with a disordered atomic structure (short-range order), in contrast to most metals, which are crystalline and have a highly ordered arrangement of atoms (long-range order). Amorphous metals are commonly referred to as “metallic glasses” or “glassy metals” and are considered to be relatively new materials with some excellent mechanical and magnetic properties. The first metallic glass was $\text{Au}_{75}\text{Si}_{25}$ alloy produced by W. Klement (Jr.), Willens and Duwez in 1960 [1] by splat-quenching of droplets of liquid state. Following that discovery, many other binary and multicomponent alloys were obtained by rapid solidification of the liquid, cooling at rates of 105 K/s to reach metastable phase and avoid nucleation of crystalline phases. A consequence of this technique referred as “melt-spinning” was that metallic glasses could only be produced in forms of ribbons, foils, or wires, in which one dimension was limited to less than one hundred micrometers in order to achieve the necessary cooling rate. The effort was to slow down the atomic diffusion processes responsible for crystallization. Further development lead to discoveries of complex alloys that can be cooled into bulk glass form up to several centimeters thick [2].

The kinetics of diffusive atomic motion in metallic amorphous material can be modeled by a dispersion of “free volume” in the liquid which is analogous to the role of “vacancies” or empty lattice sites controlling diffusive jumps of atoms in crystals. Annihilation of quenched-in free volume during thermal annealing of metallic glasses has been demonstrated either directly by dilatometry or by diffraction methods, as shown in study [3], where both quenched-in and deformation-induced free volume were measured.

The subject of this study was an amorphous $\text{Co}_{56}\text{Fe}_{16}\text{Zr}_8\text{B}_{20}$ (at. %) alloy which exhibits a relatively wide supercooled liquid region and good soft magnetic properties [4]. In previous works dealing with this alloy [5], [6] the influence of ball milling on the structure was being investigated. Mechanical alloying by high-energy ball milling is a method for materials synthesis by solid state reactions and was developed about 40 years ago. It is a simple and versatile technique to synthesize nonequilibrium materials such as amorphous phases, nanocrystalline phases, and extended solid solutions. During the milling process, powders are subjected to high energetic impact forces that lead to chemical homogenization, refinement of the particle size, disorder in the atomic structure and formation of metastable phases. In the above mentioned studies it was shown that short-time ball milling of this alloy resulted in mechanically-induced crystallization, the formation of bcc-(Fe, Co) nanocrystals embedded in an amorphous matrix, and that cryomilling of this alloy retards that crystallization. In the present work we have focused on the investigation of the structural changes within the amorphous and also crystalline phase upon heating.

2 Goals of the research project

The aim of this work is to investigate the influence of milling time on the thermal stability of an amorphous $\text{Co}_{56}\text{Fe}_{16}\text{Zr}_8\text{B}_{20}$ alloy using in-situ high-energy X-ray diffraction measurements. Particular goals can be formulated as follows:

- measure diffraction patterns of $\text{Co}_{56}\text{Fe}_{16}\text{Zr}_8\text{B}_{20}$ amorphous alloy in-situ during heating from the room temperature up to about 650 °C for the sample “as-quenched” and samples milled for various time intervals,
- obtain thermal dependences of the relative volume changes for an amorphous and a crystalline phase by fitting the integrated diffraction patterns,
- according to that investigate the influence of heating on the structural changes and growth of crystalline phases of the amorphous alloy for various milling times.

3 Experimental part

3.1 Preparation of samples

Amorphous ribbons with a nominal composition $\text{Co}_{56}\text{Fe}_{16}\text{Zr}_8\text{B}_{20}$ (at. %) were prepared by single-roller melt spinning. High-purity elements (>99.9 %) were used to prepare the starting prealloy. The as-quenched ribbons were cut into small pieces $5 \times 10 \text{ mm}^2$ and milled up for 12 h using a RETSCH PM4000 planetary ball mill. The milling was done under argon atmosphere at a ball to powder weight ratio of 31:1 with a speed of 200 rpm. Hardened steel vials and balls were used. Ball milling (BM) was interrupted each 30 min in order to cool the container in a liquid nitrogen bath. Specially designed polystyrene cover was used to suppress warming up of vials during BM. After each 2 h of milling a small amount of powder was removed for further investigations.

3.2 High-energy X-ray diffraction at BW5

High-energy X-ray diffraction (XRD) measurements were performed at the wiggler beamline BW5 of Doris positron storage ring. At this beamline the synchrotron radiation is produced by a wiggler emitting photons with energies in the range of 60 - 150 keV. The radiation with such energies has a quite high penetration depth sufficient to perform XRD experiments even on bulk samples several mm thick. Fig. 1 describes the components of which the setup at BW5 consists. All the beam guide pipes are evacuated in order to minimize losses due to air scattering.

Firstly the polychromatic photon beam is guided to a collimator, in which the tungsten plate with a hole is used to define the size and shape of the incoming beam. We were using a square-shaped opening with the cross section of 1 mm^2 . Further the beam is monochromatized using a gradient Ge-Si (111) single crystal in the monochromator.

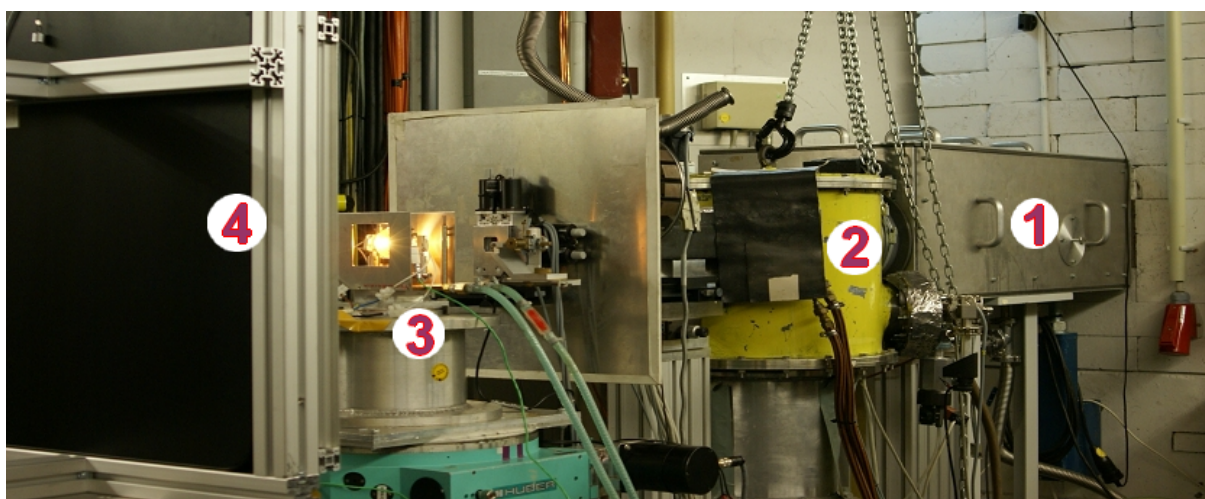


Figure 1: Beamline BW5: 1 - collimator, 2 - monochromator, 3 - placement of sample, 4 - image plate detector

Then two pairs of slits are helping to control beam profile as well as suppress air scattering. The time-controlled exposure is operated by a fast shutter. Diffracted intensity of the photons illuminating the sample is recorded by a two-dimensional image plate detector Perkin Elmer 1621 placed perpendicular to the incident beam. The detector has resolution of 2300×2300 pixels with a pixel size $150 \times 150 \mu\text{m}^2$. LaB_6 powder was used as a reference material for calibrating measurements to obtain the sample-to-detector distance.

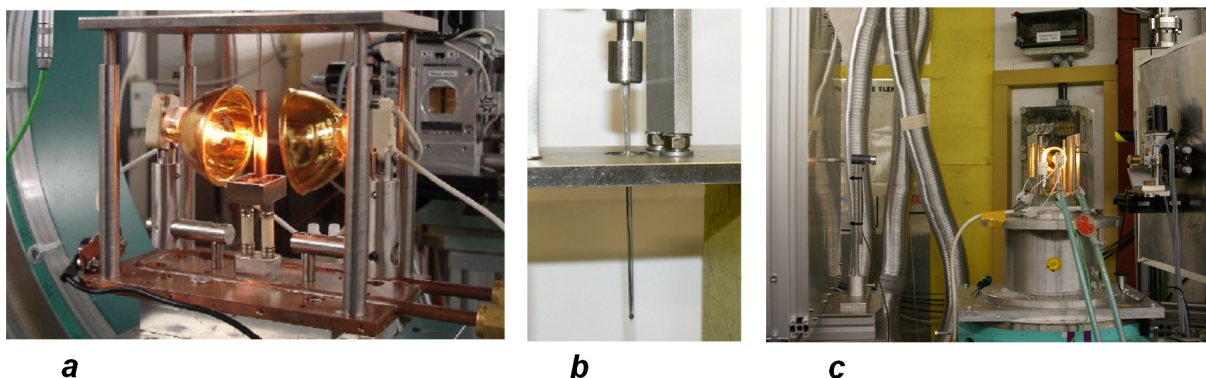


Figure 2: The tube with capillary between two lamps of the mirror infrared lamp furnace (a), detailed view on the capillary containing the sample (b), the sample placed in front of detector (c)

During our experiment the photon energy was 100 keV corresponding to a wavelength of 0.123984 \AA . Samples were put into capillaries and measured in-situ upon heating starting from the room temperature up to about 650°C . As a heater the mirror infrared lamp furnace was used and the heating rate was $10^\circ\text{C}/\text{min}$. Fig. 2 shows the tube with capillary between two lamps of the furnace, a detailed view on the capillary containing the sample and a view on the sample in front of detector, respectively.

3.3 Data treatment

Four samples of $\text{Co}_{56}\text{Fe}_{16}\text{Zr}_8\text{B}_{20}$ have been measured, the as-quenched sample (0 hours of milling) and the samples milled for 2h, 6h and 12h. A set of diffraction patterns has been obtained. Fig. 3a shows the diffraction data of an amorphous sample “as-quenched” at room temperature. The patterns are symmetric and consist of concentric rings. X-ray measurements were carried out in the wave-vector range q from 0 to 18 \AA^{-1} , $q = (4\pi\sin\theta)/\lambda$. Radial integration of the rings yields the intensity $I(q)$ versus wave-vector q curves (fig. 3b). The integration was done using the software FIT2D [7].

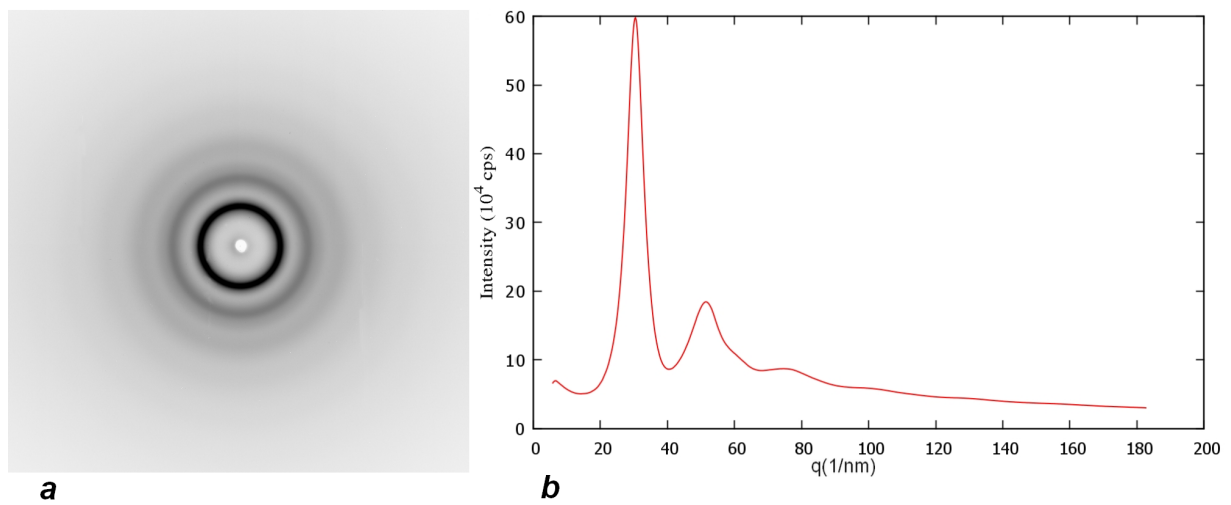


Figure 3: Diffraction data of an amorphous $\text{Co}_{56}\text{Fe}_{16}\text{Zr}_8\text{B}_{20}$ as-quenched sample at room temperature (a) and the intensity $I(q)$ versus wave-vector q obtained by radial integration (b)

Arising from the Ehrenfest relation, which yields the average interatomic separation and the important consequence, that the variation of q with temperature is inversely proportional to the mean atomic spacing, Yavari et al. [3] claimed that the third power of the position of the first, principal diffraction peak determines the volume thermal expansion of glassy structure as follows:

$$\left[\frac{q_{\max}(T_0)}{q_{\max}(T)} \right]^3 = \left[\frac{V(T)}{V(T_0)} \right] = [1 + \alpha_{th}(T - T_0)] \quad (1)$$

where α_{th} is the volume coefficient of thermal expansion below T_g as long as no structural change occurs and corresponds to the temperature slope or derivative of the reduced mean atomic volume $[V(T)/V(T_0)]$ at T , with the reference T_0 corresponding to room temperature.

In order to obtain thermal dependence of q_{\max} and consecutively of the relative volume change, we fitted the principal diffraction peak with pseudo-Voigt function and

linear background so that we got the precise position of the maximum. Pseudo-Voigt function $f_P(x)$ has the following analytical form

$$f_P(x) = A [\alpha C(x) + (1 - \alpha)G(x)], \quad (2)$$

where A is amplitude, $C(x) = (1 + x^2)^{-1}$ represents Cauchy and $G(x) = \exp[-(\ln 2)x^2]$ Gaussian part, with $x = (q - q_0/w)$, in which $2w$ is the full-width at half-maximum (FWHM), α the Cauchy content and q_0 the position of a peak maximum. Because the milled samples contain bcc-(Fe,Co) crystalline phase and the increasing temperature causes the nanocrystals grow, we used for fitting the principal peak a sum of two pseudo-Voigt functions, one for the amorphous and second for the crystalline phase (fig. 4). Then we were able to study the structural changes in both phases. The sum of two pseudo-Voigt functions was used only in case of samples milled for 6h and 12h, because in the as-quenched sample and sample milled for 2h the crystalline phase was not present or could be neglected. Finally, using relation (1) we obtained the thermal dependences of relative volume changes for the amorphous and also the crystalline phase.

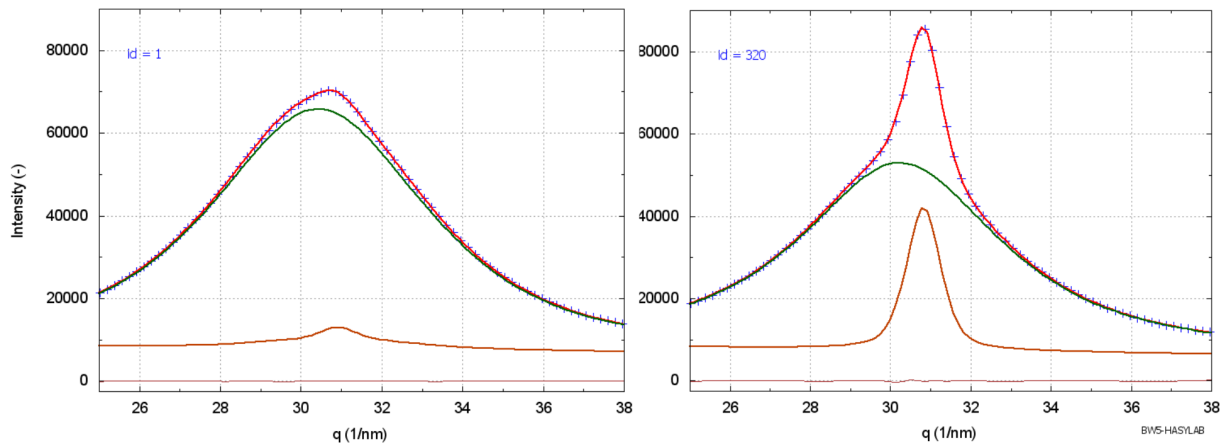


Figure 4: Fitting of the principal diffraction peak of sample milled for 6h with a sum of two pseudo-Voigt functions (red), one for the amorphous (green) and second for the crystalline phase (dark orange), at room temperature (left graph) and at 650 °C (right graph)

4 Results and Discussion

The in-situ measurements confirmed the mechanically-induced crystallization after ball cryomilling. For comparison fig. 5 shows series of XRD patterns in 3D space acquired during heating up to a temperature of 650 °C for the as-quenched sample (fig. 5a) and the sample milled for 12h (fig. 5b). In the XRD patterns the presence of bcc-(Fe,Co) nanocrystalline phase in case of samples “6h” and “12h” starts to be observable as early

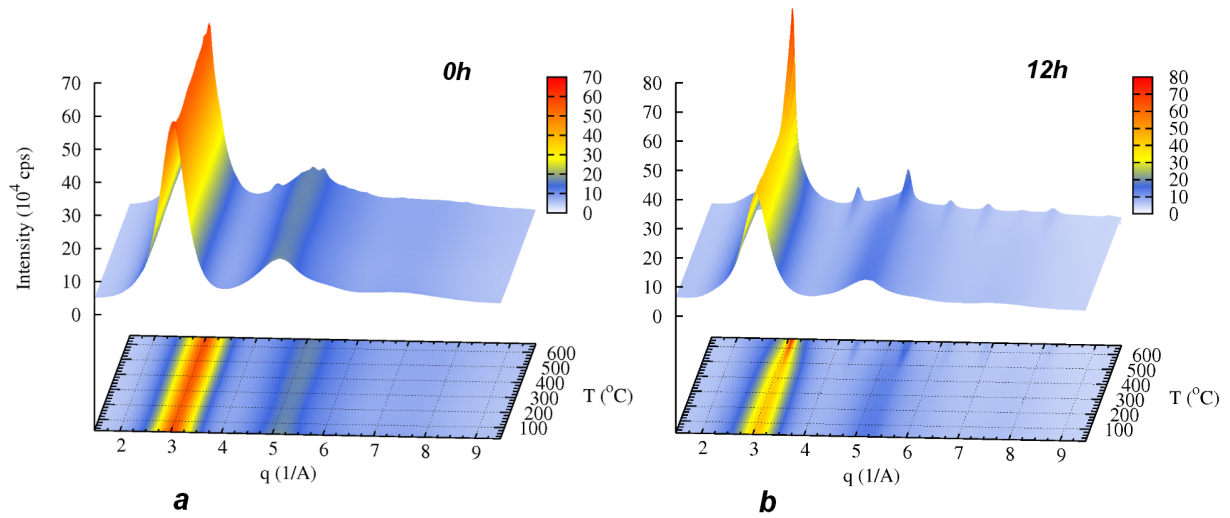


Figure 5: Series of X-ray diffraction patterns in 3D space acquired during heating for as-quenched sample (a) and sample milled for 12h (b)

as less than 400 °C is reached. The pseudo-Voigt function model of the first peak reveals the early stages of crystallization in those two samples even from the initial state.

Thermal dependences of the relative volume changes up to a temperature of 400 °C are plotted in fig. 6. Fig. 6a refers to the amorphous phase for all four samples and fig. 6b to the crystalline phase for samples milled for 6h and 12h. It can be seen that the relative volume change of the amorphous phase increases linearly with increasing temperature in case of “as-quenched” and “2h” samples but in case of “6h” and “12h” samples at a temperature about 150 °C the slopes of dependences start to be less steep. We assume that this fact is connected with the presence of crystalline phase. In an amorphous material the increase of relative volume change stands for the enlarging of the average interatomic separation. The volume coefficients of thermal expansion α_{th} of the amorphous phase were obtained from a linear fit of the slope up to a temperature of 150 °C for all samples. The values are $\alpha_{th} = 3 \times 10^{-5} 1/^{\circ}\text{C}$ for samples “0 h”, “6 h” and “12 h” and $\alpha_{th} = 2 \times 10^{-5} 1/^{\circ}\text{C}$ for the sample “2 h”. The curves showing decrease of steepness seem rather similar to those obtained by Yavari et al. [3] measured on an amorphous $\text{Pd}_{40}\text{Cu}_{30}\text{Ni}_{10}\text{P}_{20}$ alloy. He explains that “free volume” gradually disappears during heating up to a glass transition temperature T_g at which all thermo-mechanical history of the metallic glass is erased. According to DSC scan carried out in the study [6], the glass transition temperature T_g of the as-quenched $\text{Co}_{56}\text{Fe}_{16}\text{Zr}_8\text{B}_{20}$ sample was found to be 839 K (566 °C), followed by a wide super-cooled liquid region ($\Delta T_x = 50\text{K}$) and a sharp single crystallization peak at $T_{x1} = 889\text{K}$ (616 °C).

Fig. 6b shows that the relative volume change of crystalline bcc-(Fe,Co) phase increases with temperature, which means the increase of the value of lattice parameter d . An outlook for further study can be to investigate the structural changes of this

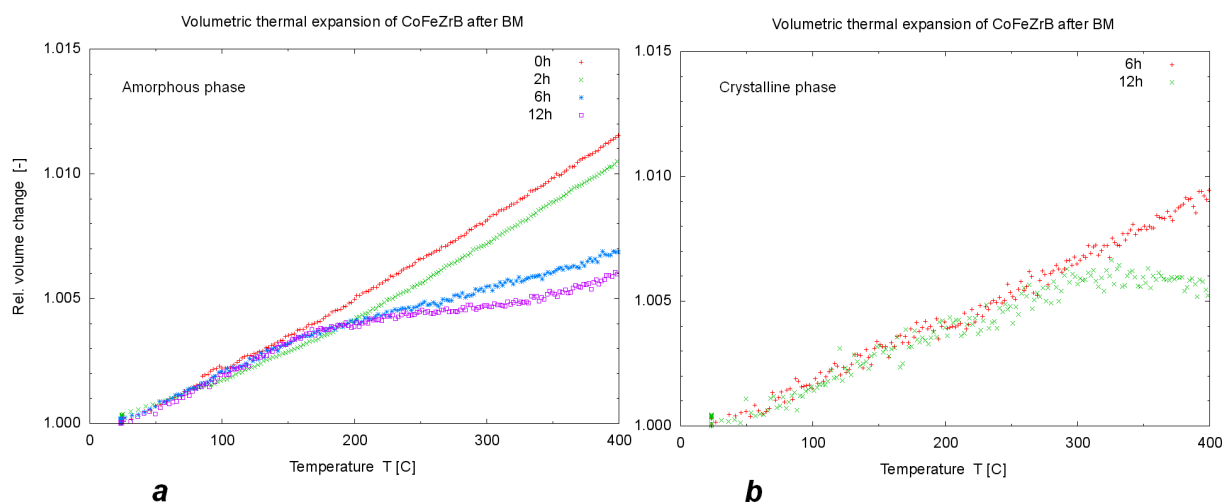


Figure 6: Thermal dependences of the relative volume changes up to a temperature of 400 °C for the amorphous phase(a) and for the crystalline phase (b)

amorphous material during heating by looking into the vicinities of atoms using EXAFS method.

5 Conclusions

The influence of milling time on thermal stability of an amorphous $\text{Co}_{56}\text{Fe}_{16}\text{Zr}_8\text{B}_{20}$ alloy has been investigated using in-situ high-energy X-ray diffraction measurements. The mechanically-induced crystallization after ball cryomilling was confirmed and the thermal dependences of relative volume changes for an amorphous and a crystalline phase were obtained. We observed that in case of samples milled for 6 h and 12 h the slopes of dependences for the amorphous phase start to be less steep at a temperature about 150 °C, in contrast to the as-quenched sample and the sample milled for 2 h which show linear thermal dependences. That indicates the relation with the presence of bcc-(Fe, Co) nanocrystals in an amorphous matrix which also show growing with the increasing temperature.

Acknowledgement

I would like to thank all people who helped me during my work at DESY, especially my supervisor Dr. Jozef Bednarčík and his PhD student Vladimír Kolesár. Last but not least, my thanks belong to DESY that allowed me to participate at the DESY Summer Student Programme 2010.

References

- [1] Klement, W., Willens, R. H., Duwez P.; *Nature* **187** (1960) 869.
- [2] Johnson, W. L.; *MRS Bull* **24** (1999) 42.
- [3] Yavari, A. R., et al.; *Acta Materialia* **53** (2005) 1611.
- [4] Inoue, A., Zhang, T., Koshiba, H., Makino, A.; *Journal of Applied Physics* **83** (1998) 6326.
- [5] Bednarčík, J., Burkel, E., Saksl, K., Kollár, P., Roth, S.; *Journal of Applied Physics*, **100** (2006) 014903.
- [6] Bednarčík, J., Saksl, K., Nicula, R., Roth, S., Franz, H.; *Journal of Non-Crystalline Solids*, **354** (2008) 5117.
- [7] Hammersley, A. P., et al.; *High Press. Res.*, **14** (1996) 235.